ARTICLES

Journal of Semiconductors
(2021) 42, 072501
doi: 10.1088/1674-4926/42/7/072501

High room-temperature magnetization in Co-doped TiO_2 nanoparticles promoted by vacuum annealing for different durations

Wenqiang Huang, Rui Lin, Weijie Chen, Yuzhu Wang, and Hong Zhang†

College of Mechanical and Electrical Engineering, Fujian Agriculture and Forestry University, Fuzhou 350002, China

Abstract: To clarify the contribution of oxygen vacancies to room-temperature ferromagnetism (RTFM) in cobalt doped TiO_2 (Co-TiO_2), and in order to obtain the high level of magnetization suitable for spintronic devices, in this work, Co-TiO_2 nanoparticles are prepared via the sol–gel route, followed by vacuum annealing for different durations, and the influence of vacuum annealing duration on the structure and room-temperature magnetism of the compounds is examined. The results reveal that with an increase in annealing duration, the concentration of oxygen vacancies rises steadily, while the saturation magnetization (M_s) shows an initial gradual increase, followed by a sharp decline, and even disappearance. The maximum M_s is as high as 1.19 emu/g, which is promising with respect to the development of spintronic devices. Further analysis reveals that oxygen vacancies, modulated by annealing duration, play a critical role in tuning room-temperature magnetism. An appropriate concentration of oxygen vacancies is beneficial in terms of promoting RTFM in Co-TiO_2. However, excessive oxygen vacancies will result in a negative impact on RTFM, due to antiferromagnetic superexchange interactions originating from nearest-neighbor Co^{2+} ions.

Key words: Co-doped TiO_2 nanoparticles; room-temperature ferromagnetism; different annealing duration; oxygen vacancy; high magnetization

Citation: W Q Huang, R Lin, W J Chen, Y Z Wang, and H Zhang, High room-temperature magnetization in Co-doped TiO_2 nanoparticles promoted by vacuum annealing for different durations[J]. *J. Semicond.*, 2021, 42(7), 072501. http://doi.org/10.1088/1674-4926/42/7/072501

1. Introduction

Due to its significant physical and chemical properties, as well as its broad application prospects in various fields, such as spintronic devices, sensors, solar cell and photocatalysis, etc., TiO_2 has garnered great attention from both academia and industry[1, 2]. This is particularly true of its possible utilization in developing spintronic devices, due to a combination of semiconducting properties and ferromagnetic features, i.e., the simultaneous utilization of both charge and spin characteristics in a single material, RTFM in TiO_2-based dilute magnetic semiconductors (DMS) has been intensively investigated both experimentally and theoretically over the past decade, since the pioneering discovery of ferromagnetism exhibited at about 400 K in cobalt-doped TiO_2 films by Matsumoto *et al.* in 2001[3].

According to the available reported results, TiO_2-based DMS include the following main categories: pristine TiO_2[4], transition metal- (Fe, Co, Mn, Ni, V, etc.) doped TiO_2[2, 5–7], rare earth- (Sm, Gd, etc.) doped TiO_2[8, 9], nonmagnetic metal- (Cu, Au, etc.) doped TiO_2[10, 11], nonmetal- (C, N, etc.) doped TiO_2[12], and TiO_2 systems, co-doped by different types of dopants[13], among which the transition metal-doped TiO_2 system has the widest appeal, owing to its notable and stable RTFM[14–18]. In particular, Co-TiO_2 DMS is considered to be the most promising candidate for the development of spintronic devices, by virtue of its remarkable ferromagnetism and stable Curie temperature at or above room temperature, as well as its simultaneous capacity for RTFM and tunable conductivity in a variety of morphologies[19–23]; as such, it has been the focus of a great deal of research[18–26].

However, the Co-TiO_2 system is deemed to be more controversial than other TiO_2-based DMS, as the room-temperature magnetism in this system, and its corresponding origins, as reported by different works, are extremely inconsistent, or even contradictory[27–31]. The debate in this issue focuses primarily on whether the RTFM of this system is an intrinsic property, originating from ferromagnetic exchange coupling between the Co ions, mediated by oxygen vacancy defects, or is driven by Co related impurity phases (Co clusters or tricobalt tetroxide) aggregated among the TiO_2 lattices.

Based on in-depth investigation, researchers incline to the viewpoint that oxygen vacancies are the decisive factor in inducing RTFM in Co-TiO_2, since an increasing number of results have demonstrated that RTFM can easily be trigged by introducing oxygen vacancy defects into the Co-TiO_2 lattice, and the RTFM is evidently enhanced, along with the concentration of oxygen vacancies[17, 31]. However, it remains an open question as to whether the RTFM in Co-TiO_2 will maintain its enhanced state with a consecutive increase in oxygen vacancies. What will the room temperature magnetism be when excessive oxygen vacancies are introduced into a Co-TiO_2 lattice? There is currently a paucity of relevant research on this issue.

Correspondence to: H Zhang, zhanghong381@fafu.edu.cn
Received 19 JANUARY 2021; Revised 3 FEBRUARY 2021.

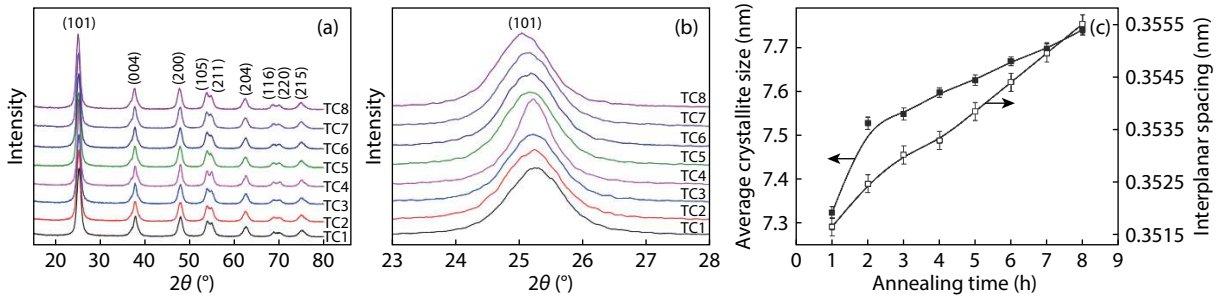

Fig. 1. (a) XRD patterns for all the samples. (b) Enlarged view of all the (101) diffraction peaks. (c) Average crystallite size, and interplanar spacing as a function of the annealing duration.

Clearly, the origin of RTFM in the Co-TiO_2 system is far from being thoroughly understood, and the influence of oxygen vacancies on RTFM should be further clarified. Moreover, the magnetism, particularly the magnetization in the Co-TiO_2 system, varies dramatically, depending on the preparation procedure and process conditions, and the reported M_s value is too low to satisfy the demand of spintronic devices. In this regard, more efforts should be devoted to addressing these two issues, so as to boost the feasible application of the Co-TiO_2 system in the development of spintronic devices.

It has been reported that annealing the samples in vacuum, i.e., under an oxygen-deficient atmosphere, is a very effective method of inducing oxygen vacancies into the TiO_2 lattice[32, 33]. Inspired by this experimental route, and with the aim of ascertaining the influence of oxygen vacancies on the room temperature magnetism in Co-doped TiO_2, in this work, Co-TiO_2 nanoparticles are prepared using a sol–gel technology, followed by vacuum annealing the samples for different durations. Vacuum annealing is anticipated to introduce oxygen vacancies into the Co-TiO_2 lattice, and different annealing durations are assumed to facilitate tuning of the oxygen vacancies' concentration, as well as the room-temperature magnetism. This work has two main objectives: the first is to further clarify the influence of oxygen vacancies on room-temperature magnetism, and the second is to achieve the high magnetization suitable for spintronic devices. The influence of oxygen vacancies on the room temperature magnetism of Co-TiO_2 nanoparticles is systematically investigated by intensively assessing the correlation between oxygen vacancies and room-temperature magnetism in Co-TiO_2 nanoparticles, and the corresponding origin for the RTFM of Co-TiO_2 nanoparticles is anticipated to finally be ascertained.

2. Experimental methods

2.1. $Ti_{0.97}Co_{0.03}O_2$ samples preparation

The nominal doping ratio of Co-TiO_2 nanoparticles is 0.03, and the component is $Ti_{0.97}Co_{0.03}O_2$; the samples were prepared using a sol–gel method similar to that reported in previous works[32–35]. A stoichiometric amount of tetra-n-butyl titanate was added into ethanol (30 mL) under continuous stirring for 30 min at room temperature to obtain the first solution. At the same time, the required quantity of $Co(NO_3)_2{\cdot}4H_2O$ was dissolved into a mixed solution, containing 28 mL ethanol, 7 mL deionized water, 0.5 mL hydrochloric acid and 20 mL acetic acid, after which the mixed solution was continuously stirred for 30 min at room temperature to obtain the second solution. The second solution was then mixed dropwise into the first solution, followed by vigorous stirring for 4 h to hydrolyze the mixed solution into a pink transparent $Ti_{0.97}Co_{0.03}O_2$ precursor sol. The purpose of adding a minute quantity of hydrochloric acid was to tune the pH value of the mixed solution, thereby controlling the hydrolysis rate.

After aging in air under ambient conditions for 72 h, the $Ti_{0.97}Co_{0.03}O_2$ precursor sol was dried in a drying oven at 100 °C for 24 h to obtain the $Ti_{0.97}Co_{0.03}O_2$ precursor gel, which was then annealed in a vacuum tube furnace, under a vacuum pressure of 11.2 Pa at 450 °C for different durations (1, 2, 3, 4, 5, 6, 7, and 8 h, respectively), and then naturally cooled to room temperature in the furnace after annealing. Finally, a set of $Ti_{0.97}Co_{0.03}O_2$ samples was obtained; the products are designated as TC1, TC2, TC3, TC4, TC5, TC6, TC7, and TC8, respectively.

2.2. $Ti_{0.97}Co_{0.03}O_2$ samples characterization

The microstructure of the all $Ti_{0.97}Co_{0.03}O_2$ samples was measured using an X-ray diffraction spectrometer (XRD, Miniflex Ⅱ) with I = 25 mA and V = 30 kV, Cu Kα radiation, and λ = 0.154056 nm. The scanning angle, 2θ, ranges from 15° to 80°, and the step size was 0.02°. The morphology images were detected using a field-emission scanning electron microscopy (FE-SEM, JSM-7401F). Raman spectra ranging from 100 to 800 cm^{-1} were recorded using a Raman spectrophotometer (DXR, Thermo Fisher) operated under an excitation source of 532 nm. The existence, as well as the various trends in the oxygen vacancy defects of all the samples was determined by means of electron paramagnetic resonance spectroscopy (EPR, Bruker). The valence state of Co and Ti ions in all the $Ti_{0.97}Co_{0.03}O_2$ samples was measured via X-ray photoelectron spectroscopy (XPS, Escalab 250Xi, Thermo Fisher). The room-temperature magnetism of the $Ti_{0.97}Co_{0.03}O_2$ samples as a function of externally applied magnetic field (M–H curves) was detected using a vibrating sample magnetometer (VSM, VersaLab magnetometer), with an externally applied magnetic field ranging from –30 to +30 kOe at room temperature.

3. Results and discussion

3.1. Microstructure and micromorphology analysis

XRD patterns for all the samples are presented in Fig. 1(a). We note that all the samples present similar XRD diffraction peaks, separately located at around 25.04°, 37.74°, 47.70°, 53.88°, 54.78°, 62.40°, 68.62°, 70.04°, and 75.02°, corres-

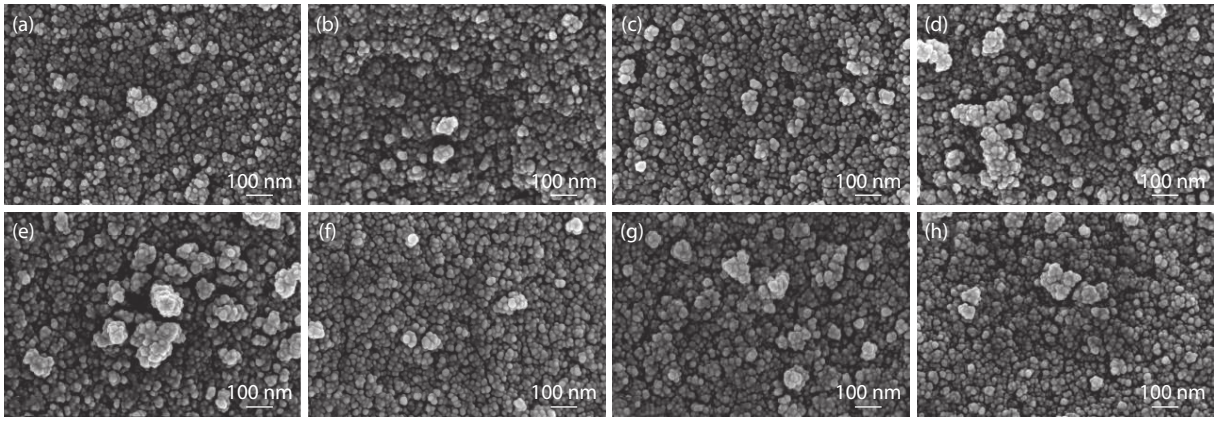

Fig. 2. SEM images for all samples.

ponding to the characteristic XRD spectra for anatase TiO_2. No impurity phases, such as rutile, metallic cobalt, oxides of cobalt, etc., are observed, indicating the satisfactory incorporation of Co ions into the TiO_2 lattice, and the monophase of anatase in all the samples. An enlarged view of the peaks for the lattice plane (101) (indexing to 25.04° angle) is provided in Fig. 1(b). This clearly shows that the (101) peaks shift gradually to lower diffraction angles with an increase in annealing duration. To further reveal the influence of annealing duration on the samples' microstructure, the average crystallite size, D, and the interplanar spacing of (101) plane, d_{101}, are calculated for all the samples, using the Scheler formula and the Bragg formula, respectively, as shown in Fig. 1(c). The results indicate that both D and d increase continuously with an increase in annealing duration, demonstrating the lattice distortion caused by annealing duration[33].

As noted in our previous work[33], oxygen vacancy defects are introduced into the lattice when TiO_2 samples are annealed under vacuum; the degree of crystallization is undermined by these defects, inducing lattice distortion. Therefore, it can reasonably be inferred that oxygen vacancies are induced in all the samples used in this work, and the concentration of oxygen vacancies will certainly increase in line with annealing duration, due to the concentration gradient of oxygen atoms between the annealing atmosphere and the samples. As has been demonstrated theoretically[36, 37], oxygen vacancies in the TiO_2 lattice will cause relaxation of Ti–Ti and Ti–O bonds, owing to the outward movement of Ti atoms to strengthen the bonding of Ti–Ti and Ti–O; thus the lattice expands gradually with the increase in oxygen vacancies, and the crystallinity of the samples is gradually distorted. Santara *et al.*[38] also observed similar lattice expansion and crystallinity distortion in a TiO_2 lattice, caused by the presence of oxygen vacancies.

The micromorphology for the samples is presented in Fig. 2. We find that all the samples exhibit similar morphology, and are composed of a large number of particles, and the micromorphology is nearly spherical, with diameters ranging from around 7 to 10 nm, comparable to the crystallite size calculated based on the XRD data. The SEM patterns confirm that Co-TiO_2 nanoparticles have been successfully synthesized.

3.2. Raman scattering analysis

Raman spectra for all the samples are shown in Fig. 3. It

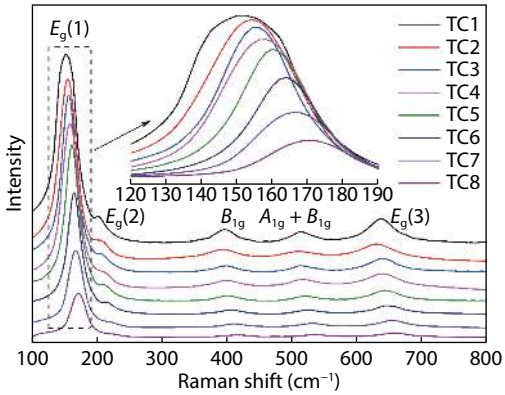

Fig. 3. Raman spectra for all samples. The inset shows an enlarged view of all the $E_g(1)$ Raman peaks.

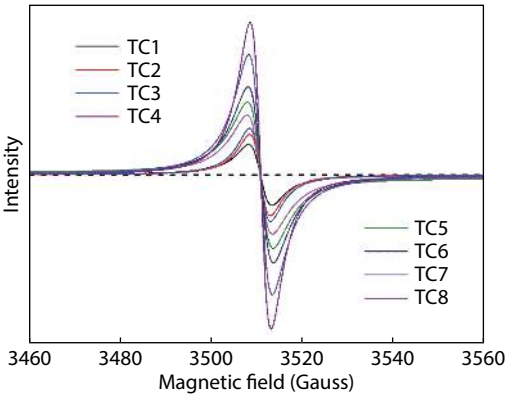

Fig. 4. EPR spectra for all samples.

is evident that all the samples exhibit similar Raman behaviors, with five Raman scattering peaks, approximately centered at 151.06, 199.48, 395.80, 513.12, and 635.57 cm^{-1}, respectively. All these Raman scattering peaks respectively correspond to the Raman active modes of $E_g(1)$, $E_g(2)$, B_{1g}, A_{1g}, and $E_g(2)$ for anatase TiO_2[39]. No other Raman peaks assigned to rutile, metallic cobalt, or oxides of cobalt are observed from the Raman spectra, confirming the monophase of anatase in all the samples, and impurity phases, with specific reference to Co-related clusters, or tricobalt tetroxide in the TiO_2 lattices, can be ruled out. Furthermore, the Raman spectra indicate that the intensity of all the Raman scattering peaks is reduced gradually relative to annealing duration, signifying that the crystallinity of the samples is gradually dam-

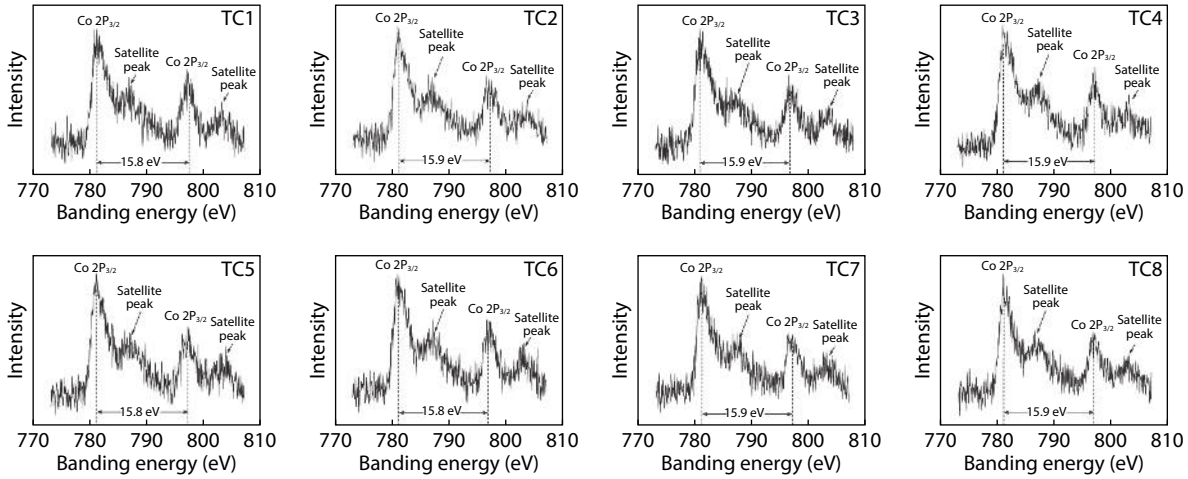

Fig. 5. Core level XPS spectra of Co 2p for all samples.

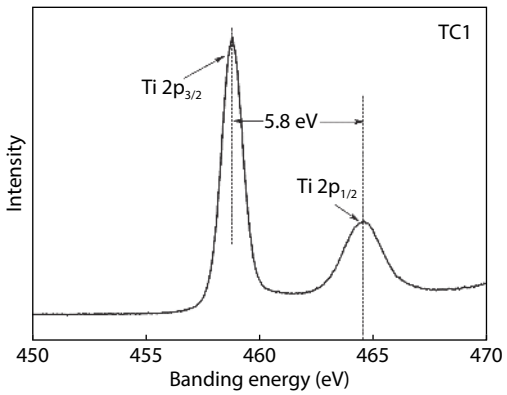

Fig. 6. Core level XPS spectrum of Ti 2p for the TC1 sample.

aged with the increase in annealing duration, which is consistent with the results shown in the XRD patterns.

It has been demonstrated that the $E_g(1)$ mode located at 151.06 cm^{-1} is extremely sensitive to the oxygen vacancy defects in the TiO_2 lattice, and that variations in oxygen vacancy concentration can be deduced based on the shift in this scattering peak[30–33]. Here, we observe that the $E_g(1)$ mode of the Co-TiO_2 samples exhibits blue shift towards high Raman shift, as shown in the inset of Fig. 3, indicating that the oxygen vacancy concentration steadily increases in line with vacuum annealing duration. Combining the results and analysis of both XRD and Raman scattering, we can conclude that vacuum annealing duration has a significant impact on the microstructure of the Co-TiO_2 samples.

3.3. EPR results analysis

To further corroborate the influence of vacuum annealing duration on variations in oxygen vacancy concentrations, EPR spectra for the samples were obtained via electron paramagnetic resonance spectroscopy, and are shown in Fig. 4. All the samples exhibit similar EPR behavior, with *g*-values of $g \approx 2.005$, indicating the presence of oxygen vacancy defects in all the samples. Moreover, as discussed in our previous work[33], the intensity of the EPR signal resulting from oxygen vacancies is indicative of the concentration of oxygen vacancies in the TiO_2 lattice.

We can therefore assert, based on the variation in the intensity of the EPR peaks, that the concentration of oxygen vacancies in the Co-TiO_2 lattice rises steadily with vacuum annealing duration, with the TC8 sample having the highest concentration of oxygen vacancies, while that in TC1 is the lowest. As such, the variation trend in the oxygen vacancies content inferred from XRD and Raman scattering results is confirmed.

3.4. XPS analysis

The chemical state of Co and Ti elements in the Co-TiO_2 lattice is determined via X-ray photoelectron spectroscopy, and the core level XPS spectra for Co 2p are presented in Fig. 5. This shows that there are two main XPS peaks, separately located at 781.03 and 796.88 eV, corresponding to the core level Co $2p_{3/2}$, and Co $2p_{1/2}$, respectively. The difference in the binding energy for these two XPS peaks is 15.8 or 15.9 eV in all the samples, indicating that the chemical state of Co in all the Co-TiO_2 samples is the divalent state of Co^{2+}[16].

Meanwhile, two extra XPS peaks, located at 786.69 and 803.01 eV, are observed in the XPS spectra, which are respectively ascribed to the resonant shake-up satellite peaks for the multiplet of Co $2p_{3/2}$ and Co $2p_{1/2}$, further demonstrating the divalent state of Co^{2+} in all the as-synthesized samples[40, 41]. It has been reported that the XPS peak for metallic Co $2p_{3/2}$ is located approximately at 778.3 eV[31, 41], but no obvious signal corresponding to this peak is detected here, and as such, the presence of metallic Co clusters in all the samples can be ruled out, and the incorporation of Co into the TiO_2 lattice in the divalent state of Co^{2+} is confirmed.

The core-level XPS spectrum of Ti 2p for the TC1 sample is presented in Fig. 6. It is apparent that two main XPS peaks separately center at banding energies of 458.7 and 464.5 eV, which are indexed to Ti $2p_{3/2}$, and Ti $2p_{1/2}$, respectively. The banding energy difference between these two peaks is 5.8 eV, indicating the tetravalent state of Ti^{4+} in TC1[31]. The XPS spectra of the remaining samples are similar to that of TC1, indicating the presence of tetravalent Ti^{4+} in all the samples.

The radius of Co^{2+} (7.5×10^{-11} m) is larger than that of Ti^{4+} (6.1×10^{-11} m), but small variations in d_{101}, impacted by increasing annealing duration, is observed in the XRD analysis, indicating that most of the Co^{2+} ions are located in the interstitial sites or on the surface[31]. Since the bond length of Ti–O in standard anatase ($(1.934–1.980) \times 10^{-10}$ m) is much larger

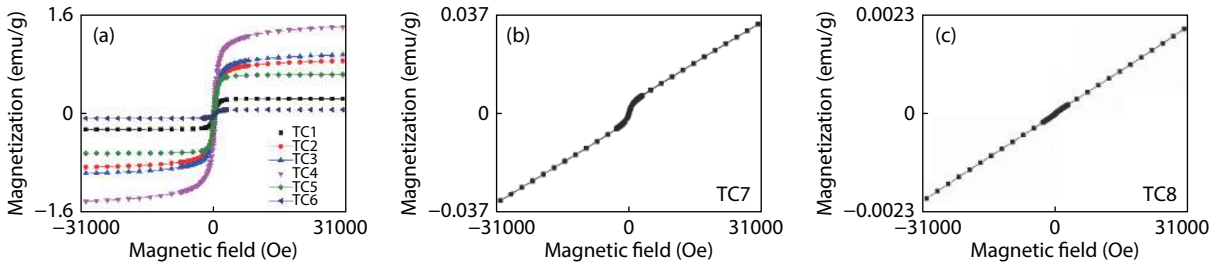

Fig. 7. Room-temperature hysteresis loops for all samples: (a) TC1, TC2, TC3, TC4, TC5, TC6, (b) TC7, (c) TC8.

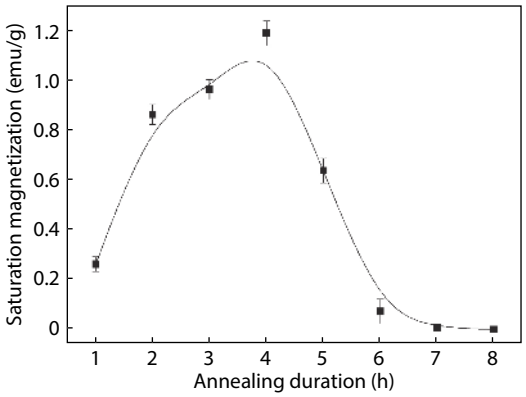

Fig. 8. Saturation magnetization as a function of annealing duration for all samples.

than the radius of Co^{2+}, it can reasonably be inferred that more and more interstitial Co^{2+} will gather together, due to the recombination and relaxation of Ti–Ti and Ti–O bonds caused by the outward movement of Ti atoms, as revealed in the XRD analysis; as such, the distance between neighboring Co^{2+} ions will be reduced.

3.5. Room-temperature magnetism analysis

Magnetization as a function of the external magnetic field (*M*–*H* curve), ranging from −30 to +30 kOe at room temperature for all the samples, is displayed in Fig. 7. It is apparent in Fig. 7(a) that the TC1, TC2, TC3, TC4, TC5, and TC6 samples possess the typical magnetic hysteresis loop, with the magnetization saturating under a high magnetic field, demonstrating the occurrence of ferromagnetism at room temperature in these samples. Conversely, the magnetization of the TC7 sample rises sharply with the external magnetic field without any sign of saturation, even under a magnetic field of up to 30 kOe, as shown in Fig. 7(b), which indicates the coexistence of paramagnetic phase and a fraction of ferromagnetic phase in the TC7 sample. The magnetic property of TC7 is similar to that reported in previous work[32]. With regard to the TC8 sample, the magnetization linearly increases with the external magnetic field, as shown in Fig. 7(c), which is a clear demonstration of room-temperature paramagnetism in the TC8 sample.

It can therefore be concluded that the room temperature magnetism of the Co-TiO_2 nanoparticles is significantly influenced by vacuum annealing duration. When vacuum-annealed for a short duration, less than or equal to 6 h, Co-TiO_2 nanoparticles exhibit RTFM, with the M_s value varying significantly with the increase in annealing duration. The M_s shows an initial gradual increases in line with the annealing duration, and reaches a maximum of 1.19 emu/g when vacuum annealed for 4 h, and then sharply declines with a further increase in annealing duration, as shown in Fig. 8. On extending the annealing duration beyond 6 h, the RTFM rapidly weakens, but paramagnetism raises dramatically, and the RTFM eventually undergoes a complete transformation into paramagnetism, based on increased annealing duration. In addition, the maximum M_s obtained in this work is far higher than the reported results[16, 17, 30, 31, 42]. From perspective of the application of DMS in spintronic devices, enhanced RTFM, and, in particular, strong M_s, are among the desired properties pursued by researchers[1, 43]. In this regard, the maximum M_s obtained here is a promising value with respect to the potential development of spintronic devices.

According to the analysis above, we conclude that vacuum annealing for different durations is an extremely effective approach to tuning room temperature magnetization, as well as the concentration of lattice defects, in particular the oxygen vacancy content of Co-TiO_2 nanoparticles. Moreover, it can be deduced from the analysis that there must be a connection between RTFM and oxygen vacancies in Co-TiO_2 nanoparticles. The RTFM is initially enhanced with the increased oxygen vacancy concentration, and then sharply declines, even disappears, with a further increase in the concentration of oxygen vacancies. It can therefore reasonably be inferred that oxygen vacancies, modulated by annealing duration, play a critical role in tuning room-temperature magnetism, since no impurity phase is present in the samples, and oxygen vacancy defects are the sole endogenous variable affecting the level of room-temperature magnetism.

As has been demonstrated, Co^{2+} ions are apt to align with neighboring Co^{2+} ions, coupling via oxygen vacancies to form bound magnetic polarons (BMPs), and triggering ferromagnetic exchange interaction; hence, RTFM occurs in Co-TiO_2 nanoparticles[28]. Accordingly, RTFM in Co-TiO_2 nanoparticles will certainly be sustainably enhanced by an increase in oxygen vacancies.

Nevertheless, an excessive oxygen vacancy content will reduce the distance between neighboring Co^{2+} ions, owing to the lattice distortion caused by oxygen vacancy defects, as revealed in the XRD and XPS results; the nearest neighboring Co^{2+} ions will therefore couple with each other to form Co^{2+}–Co^{2+}, giving rise to antiferromagnetic super exchange interaction between Co^{2+} ions[31]. As such, the RTFM will decline or even disappear with further increases in oxygen vacancies, due to the strengthening of antiferromagnetic superexchange interaction, and paramagnetism is consequently induced in the Co-TiO_2 nanoparticles. To summarise, appropriate concentration of oxygen vacancies is beneficial in terms of promoting RTFM in Co-TiO_2 nanoparticles, while an excess-

ive oxygen vacancy content will result in a negative impact on RTFM, inducing paramagnetism.

4. Conclusion

In conclusion, in this work, a series of Co-TiO_2 nanoparticles were successfully prepared by a sol–gel route, followed by vacuum annealing of the resulting samples for different durations. The contribution of oxygen vacancies to room-temperature magnetism in the Co-TiO_2 system has been systematically clarified by investigating the influence of different annealing duration on oxygen vacancy defects, as well as on magnetism. Our four conclusions can be summarized as follows:

(1) Vacuum annealing for different durations is a very effective method of tuning the concentration of oxygen vacancies and RTFM in a Co-TiO_2 system.

(2) Oxygen vacancies play a critical role in generating room temperature magnetism. An appropriate concentration of oxygen vacancies is beneficial for promoting RTFM in Co-TiO_2. However, excessive oxygen vacancies cause room-temperature magnetism to transform from ferromagnetism into paramagnetism.

(3) Vacuum annealing for 4 h is the ideal annealing duration required to obtain high RTFM in Co-TiO_2 nanoparticles.

(4) The maximum M_s of 1.19 emu/g obtained in this work is a promising value with respect to the future development of spintronic devices.

Acknowledgements

This work was supported by the National Training Program of Innovation and Entrepreneurship for Undergraduates (No. 201910389022).

References

[1] Yakout S M. Spintronics: Future technology for new data storage and communication devices. J Supercond Nov Magn, 2020, 33, 2557

[2] Chen Z, Zhao Y S, Ma J Q, et al. Detailed XPS analysis and anomalous variation of chemical state for Mn- and V-doped TiO_2 coated on magnetic particles. Ceram Int, 2017, 43(18), 16763

[3] Matsumoto Y, Murakami M, Shono T, et al. Room-temperature ferromagnetism in transparent transition metal-doped titanium dioxide. Science, 2001, 291(5505), 854

[4] Bolokang A S, Cummings F R, Dhonge B P, et al. Characteristics of the mechanical milling on the room temperature ferromagnetism and sensing properties of TiO_2 nanoparticles. Appl Surf Sci, 2015, 311, 362

[5] Choudhury B, Verma R, Choudhury A. Oxygen defect assisted paramagnetic to ferromagnetic conversion in Fe doped TiO_2 nanoparticles. RSC Adv, 2014, 4(55), 29314

[6] Tian J J, Gao H P, Deng H M, et al. Structural, magnetic and optical properties of Ni-doped TiO_2 thin films deposited on silicon (100) substrates by sol–gel process. J Alloy Compd, 2013, 581(13), 318

[7] Semisalova A S, Mikhailovsky Y O, Smekhova A, et al. Above room temperature ferromagnetism in Co- and V-doped TiO_2 — revealing the different contributions of defects and impurities. J Supercond Nov Magn, 2015, 28(3), 805

[8] Tseng L T, Luo X, Li S, et al. Magnetic properties of Sm-doped rutile TiO_2 nanorods. J Alloy Compd, 2016, 687, 294

[9] Paul S, Choudhury B, Choudhury A. Magnetic property study of Gd doped TiO_2 nanoparticles. J Alloy Compd, 2014, 601, 201

[10] Xu N N, Li G P, Lin Q L, et al. Structural and magnetic study of undoped and Cu-doped rutile TiO_2 single crystals. J Supercond Nov Magn, 2017, 30(9), 2591

[11] Zou Z R, Zhou Z P, Wang H Y, et al. Effect of Au clustering on ferromagnetism in Au doped TiO_2 films: theory and experiments investigation. J Phys Chem Solids, 2017, 100, 71

[12] Wang J B, Wu K C, Mi J W, et al. Room-temperature ferromagnetism in carbon- and nitrogen-doped rutile TiO_2. Appl Phys A, 2015, 118(2), 725

[13] Wei G D, Wei L, Chen Y X, et al. Magnetic coupling and electric transport in Nb, Fe co-doped rutile TiO_2 epitaxial films. J Alloy Compd, 2017, 695, 2261

[14] Ahmed S A. Annealing effects on structure and magnetic properties of Mn-doped TiO_2. J Magn Magn Mater, 2016, 402, 178

[15] Ahmed S A. Ferromagnetism in Cr-, Fe-, and Ni-doped TiO_2 samples. J Magn Magn Mater, 2017, 442, 152

[16] Chanda A, Rout K, Vasundhara M, et al. Structural and magnetic study of undoped and cobalt doped TiO_2 nanoparticles. RSC Adv, 2018, 8(20), 10939

[17] Stella C, Prabhakar D, Prabhu M, et al. Oxygen vacancies induced room temperature ferromagnetism and gas sensing properties of Co-doped TiO_2 nanoparticles. J Mater Sci-Mater Electron, 2016, 27(2), 1636

[18] Lin Y B, Yang Y M, Zhuang B, et al. Ferromagnetism of Co-doped TiO_2 films prepared by plasma enhanced chemical vapour deposition (PECVD) method. J Phys D, 2008, 41(19), 195007

[19] Cortie D L, Khaydukov Y, Keller T, et al. Enhanced magnetization of cobalt defect clusters embedded in $TiO_{2-\delta}$ films. ACS Appl Mater Inter, 2017, 9(10), 8783

[20] Santara B, Pal B, Giri P K, et al. Signature of strong ferromagnetism and optical properties of Co doped TiO_2 nanoparticles. J Appl Phys, 2011, 110(11), 114322

[21] Griffin R K, Varela M, Rashkeev S, et al. Defect-dediated ferromagnetism in insulating Co-doped anatase TiO_2 thin films. Phys Rev B, 2008, 78(1), 014409

[22] Shinde S R, Ogale S B, Higgins J S, et al. Co-occurrence of superparamagnetism and anomalous Hall effect in highly reduced cobalt-doped rutile $TiO_{2-\delta}$ films. Phys Rev Lett, 2004, 92(16), 166601

[23] Bryan J D, Santangelo S A, Keveren S C, et al. Activation of high-TC ferromagnetism in Co^{2+}:TiO_2 and Cr^{3+}:TiO_2 nanorods and nanocrystals by grain boundary defects. J Am Chem Soc, 2005, 127(44), 15568

[24] Srinivas K, Reddy P V. Synthesis, structural, and magnetic properties of nanocrystalline $Ti_{0.95}Co_{0.05}O_2$-diluted magnetic semiconductors. J Supercond Nov Magn, 2014, 27(11), 2521

[25] Kaushik A, Dalela B, Kumar S, et al. Role of Co doping on structural, optical and magnetic properties of TiO_2. J Alloy Compd, 2013, 552, 274

[26] Sharma S, Thakur N, Kotnala R K, et al. Structure and magnetic properties of $Ti_{1-x}Co_xO_2$ nanoparticles prepared by chemical route. J Cryst Growth, 2011, 321(1), 19

[27] Kumar S, Park J S, Kim D J, et al. Electronic structure and magnetic properties of Co doped TiO_2 thin films using X-ray absorption spectroscopy. Ceram Int, 2015, 41(Supplement 1), S370

[28] Shinde S R, Ogale S B, Sarma S D, et al. Ferromagnetism in laser deposited anatase $Ti_{1-x}Co_xO_{2-\delta}$ films. Phys Rev B, 2003, 67(11), 115211

[29] Karthik K, Pandian S K, Kumar K S, et al. Influence of dopant level on structural, optical and magnetic properties of Co-doped anatase TiO_2 nanoparticles. Appl Surf Sci, 2010, 256(14), 4757

[30] Tseng L T, Luo X, Tan T T, et al. Doping concentration dependence of microstructure and magnetic behaviours in Co-doped TiO_2 nanorods. Nanoscale Res Lett, 2014, 9, 673

[31] Choudhury B, Choudhury A, MaidulIslam A K M, et al. Effect of oxygen vacancy and dopant concentration on the magnetic properties of high spin Co^{2+} doped TiO_2 nanoparticles. J Magn Magn Ma-

ter, 2011, 323(5), 440
[32] Zhang H, Chen M X, Wang Y Z, et al. Correlation between oxygen vacancies and room temperature ferromagnetism in $Ti_{0.94}Co_{0.03}La_{0.03}O_2$ nanoparticles influenced by different post annealing treatment. J Sol–gel Sci Techn, 2018, 86(1), 162
[33] Zhang H, Huang W Q, Lin R, et al. Room temperature ferromagnetism in pristine TiO_2 nanoparticles triggered by singly ionized surface oxygen vacancy induced via calcining in different air pressure. J Alloy Compd, 2021, 860, 157913
[34] Zhang H, Zheng L Q, Ouyang X H, et al. Carbon doping of $Ti_{0.91}Co_{0.03}La_{0.06}O_2$ nanoparticles for enhancing room-temperature ferromagnetism using carboxymethyl cellulose as carbon source. Ceram Int, 2018, 44(13), 15754
[35] Zhang H, Xu Y, Yang W B, et al. Structural and magnetic evolution of Fe-doped TiO_2 nanoparticles synthesized by sol–gel method. J Electroceram, 2017, 38(1), 104
[36] Lee H Y, Clark S J, Robertson J. Calculation of point defects in rutile TiO_2 by the screened-exchange hybrid functional. Phys Rev B, 2012, 86(7), 075209
[37] Na-Phattalung S, Smith M F, Kim K, et al. First-principles study of native defects in anatase TiO_2. Phys Rev B, 2006, 73(12), 125205
[38] Santara B, Giri P K, Dhara S, et al. Oxygen vacancy-mediated enhanced ferromagnetism in undoped and Fe-doped TiO_2 nanoribbons. J Phys D, 2014, 47(73), 235304
[39] Patel S K S, Gajbhiye N S, Date S K. Ferromagnetism of Mn-doped TiO_2 nanorods synthesized by hydrothermal method. J Alloy Compd, 2011, 509(S1), S427
[40] Mahmoud M S, Ahmed E, Farghalid A A, et al. Synthesis of Fe/Co-doped titanate nanotube as redox catalyst for photon-induced water splitting. Mater Chem Phys, 2018, 217, 125
[41] Yadav H M, Kim J S. Sol–gel synthesis of Co^{2+}-doped TiO_2 nanoparticles and their photocatalytic activity study. Sci Adv Mater, 2017, 9(12), 1114
[42] Kumar A, Kashyap M K, Sabharwal N, et al. Structural, optical and weak magnetic properties of Co and Mn codoped TiO_2 nanoparticles. Solid State Sci, 2017, 73, 19
[43] Li Z H, Zhong W W, Li X M, et al. Strong room-temperature ferromagnetism of pure ZnO nanostructure arrays via colloidal template. J Mater Chem C, 2013, 1(41), 6807

Wenqiang Huang is currently a undergraduate in College of Mechanical and Electrical Engineering, Fujian Agriculture and Forestry University. He is the project principal of the National Training Program of Innovation and Entrepreneurship for Undergraduates (No. 201910389022) under the supervision of Dr Hong Zhang. His current research focuses on the magnetic performance of TiO_2-based dilute magnetic semiconductor.

Hong Zhang got his PhD from Fujian Agriculture and Forestry University. He worked in Limerick Pulp and Paper Centre, University of New Brunswick, Canada as a visiting scholar from 2017 to 2018. He is currently an associate professor in College of Mechanical and Electrical Engineering, Fujian Agriculture and Forestry University. His current research focuses on the magnetic performance of TiO_2-based dilute magnetic semiconductor.